doi.org/10.36721/PJPS/2026.40.16003.1

Exploring the association of quercetin with liver fibrosis through network pharmacology and 16S rRNA gene sequencing

Ruiqi Zhao[1#], Xiaowen Song[1#], Mingkai Qin[1], Bingxuan Fan[1], Shufang Niu[1], Donghua Zheng[1], Jiali Liu[1], Jun Qi[2], Peng Wang[3], Jianfang Sun[2], Feng Bai[2]* and Wanfu Bai[1]*

[1]Baotou Medical College, Inner Mongolia 014000, China
[2]The First Affiliated Hospital of Baotou Medical College, Baotou, China
[3]The Second Affiliated Hospital of Baotou Medical College, Baotou, China

Abstract: **Background**: Liver fibrosis is a chronic wound healing process of liver injury and gut–liver axis dysregulation has been recently identified as an important contributor to liver fibrosis progression. Quercetin has been reported to have anti-inflammatory activity and microbiota-modulating effects. However, the potential targets of quercetin remain unclear, as does the relationship between quercetin-associated targets and changes in the gut microbiota in liver fibrosis. **Objectives**: The purpose of this study was to use network pharmacology to predict potential targets of quercetin associated with liver fibrosis and to explore changes in gut microbiota following treatment with quercetin using a CCl_4-induced rat model. **Methods**: Eighteen male Sprague–Dawley rats were randomized into CON group, MOD group and QR group (n = 6 per group). Liver fibrosis was induced by weekly subcutaneous injection of carbon tetrachloride (CCl_4) for eight weeks. Oral gavage of quercetin (50 mg/kg/day) was performed in QR group. Histopathological changes were assessed by hematoxylin–eosin staining, Masson staining and Ishak scoring. Potential targets of quercetin were screened using network pharmacology, followed by protein–protein interaction (PPI) network construction and Gene Ontology (GO)/Kyoto Encyclopedia of Genes and Genomes (KEGG) enrichment analyses. Cecal microbiota composition was determined by 16S rRNA gene sequencing. Parametric or non-parametric tests were used accordingly, including one-way ANOVA or Kruskal–Wallis test. **Results**: Histopathology revealed significant liver injury and fibrosis in the MOD group relative to the CON group. The QR group showed lower Ishak fibrosis scores and milder histopathological features compared with the MOD group. Network pharmacology analysis identified UBC, UBE2I, RBX1, PSMB7 and UBA1 as hub targets, with KEGG pathways of interest including the TNF signaling pathway, p53 signaling pathway, Toll-like receptor signaling pathway and ubiquitin-mediated proteolysis. Alpha diversity of the cecal microbiota differed significantly among groups, whereas beta diversity did not. Relative abundance of Proteobacteria decreased and Firmicutes increased in the QR group relative to the MOD group. Taxa enrichment analysis identified enrichment of *Muribaculaceae* and *Ligilactobacillus* in the QR group. **Conclusion**: Histopathology and microbiome analyses indicated that quercetin intervention was associated with altered liver histopathological features and shifts in gut microbiota composition in rats with CCl_4-induced liver fibrosis. Network pharmacology predicted several hub targets and pathways potentially linked to these observations. As the present analyses are purely correlational and lack mechanistic validation at the molecular level, no causal relationships are implied between the predicted targets/pathways and the observed histological or microbiome changes. These findings should be regarded as hypothesis-generating and warrant further validation studies.

Keywords: 16S rRNA gene sequencing; Gut microbiome; Liver fibrosis; Quercetin

Submitted on 12-01-2026 – Revised on 21-04-2026 – Accepted on 25-04-2026

Article in Press

INTRODUCTION

Liver fibrosis (LF) is a typical result of chronic liver injury and participates in the pathophysiology of nearly all chronic liver diseases. Persistent hepatic inflammation, immune abnormalities, oxidative stress and aberrant accumulation of extracellular matrix elicit hepatic stellate cell (HSC) activation, which causes fibrosis (Ying *et al*., 2026). Ultimately, severe fibrosis can lead to cirrhosis, liver failure and hepatocellular carcinoma. Thus, discovering interventions that can halt or postpone fibrosis is vital (Zhang *et al*., 2026).

Quercetin, a bioactive flavonol present in numerous medicinal plants and dietary supplements, has been shown to have various biological effects, including anti-inflammatory, antioxidant, antiviral, antihypertensive and anti-apoptotic properties (Barazesh *et al*., 2026). Quercetin was also found to correlate with protection against liver injury through regulating inflammatory responses, oxidative stress, autophagy and bile acid metabolism (Li *et al*., 2025). For instance, quercetin could downregulate the expression of sodium taurocholate co-transporting polypeptide (NTCP), thereby reducing hepatic bile acid uptake and alleviating bile acid–induced liver injury (Chen *et al*., 2025). Furthermore, recent studies have indicated

**Corresponding author:* e-mail: 765558334@qq.com; bwf007007@sina.com
#These authors contributed equally and are the co-first authors.

that quercetin may help regulate HSC activation and collagen deposition in LF. The specific molecules involved and the extensive regulatory network implicated in these processes require further clarification (Liu *et al*., 2025).

Emerging evidence also indicates that gut microbiota dysbiosis participates in the development and progression of LF. The gut–liver axis (GLA) refers to the bidirectional communication between intestinal microbes and the liver via microbial metabolites, immune factors and the portal circulation system (He *et al*., 2025). The intestinal microbes could regulate liver inflammation, immune responses and fibrosis-associated signaling pathways (Li *et al*., 2025). Gut microbiota dysbiosis has been identified in various diseases and could be potentially altered by therapeutic approaches (Shen *et al*., 2025). Alterations of gut microbiota were also reported after quercetin intervention. However, whether gut microbiota dysbiosis and the histopathological changes induced by quercetin treatment are associated in LF remains elusive. Network pharmacology is an effective approach for predicting potential targets and pathways in natural products and TCMs (Zhai *et al*., 2025). On the other hand, 16S rRNA gene sequencing could help characterize microbiota community shift under various physiological and pathological states. Network pharmacology and 16S rRNA gene sequencing have each been applied separately to investigate quercetin in liver diseases. However, it remains unclear whether the host molecular targets and signaling pathways predicted by network pharmacology overlap with the biological processes altered by quercetin-induced shifts in the gut microbiota in the context of liver fibrosis. To address this precise gap, the present study integrated network pharmacology with 16S rRNA gene sequencing in a CCl_4-induced rat model of liver fibrosis. This integrative approach was designed as a strictly hypothesis-generating analysis to explore potential correlations and overlapping biological processes between quercetin-associated host targets/pathways and microbiota alterations, without inferring any causal relationships.

MATERIALS AND METHODS

Drugs and reagents

Quercetin was bought from Tianjin Chemical Factory (Tianjin, China). Carbon tetrachloride (CCl4, lot No. 20091217) was purchased from Tianjin Chemical Factory. Extra virgin olive oil (batch No. 20150123) was provided by Shandong Luhua Group Co., Ltd. Ultrapure water was acquired from Sigma (USA). Chromatography-grade formic acid was bought from Dikma Technologies (USA).

Animals and experimental design

18 male Sprague–Dawley (SD) rats (Age: 4 weeks, weight:170–200 g, SPF grade) were purchased from the Experimental Animal Science Department. Temperature (23–25 °C), relative humidity (50 ± 5%) and lighting (12 h light/dark cycle) were controlled automatically and rats had free access to water and standard chow diet throughout the experimental period. Only male rats were used to avoid hormone changes in female rats that could affect the results, as hormones are known to alter liver metabolism, immune tolerance, inflammation, and the composition of the gut microbiota in experimental models of fibrosis.

Animal care and experiments were performed in accordance with the standards of the institutional animal care and use committee. Animals were randomly divided into the following 3 groups (n = 6 in each group): CON group, MOD group and QR group. To minimize potential cage effects in the microbiome analysis, rats from different treatment groups were housed in separate cages (2–3 rats per cage) under identical environmental conditions. A liver fibrosis model was established by injecting CCl_4 dissolved in olive oil subcutaneously as described in the literature. The QR group was administered quercetin (50 mg/kg/day, oral gavage) and the dosage used was based on the previous study.

Network pharmacology analysis

Identification of quercetin targets

Potential molecular targets of quercetin were obtained from the Traditional Chinese Medicine Systems Pharmacology Database (TCMSP) (Ru *et al*., 2014). The three-dimensional structure of quercetin was retrieved from the PubChem database (Kim *et al*., 2023) and uploaded to PharmMapper for target prediction based on pharmacophore mapping (Wang *et al*., 2017). Predicted targets were standardized using the UniProt database to convert protein identifiers to official gene symbols and to exclude non-human targets (Feuermann *et al*., 2025). Duplicate targets were removed to generate the final list of candidate targets.

Identification of liver fibrosis-related targets

Liver fibrosis-associated genes were collected from the GeneCards and OMIM databases using the keyword “liver fibrosis” (Qiang *et al*., 2022). Targets with relevance to liver fibrosis were integrated and duplicate entries were removed. Common targets between quercetin and liver fibrosis were identified using Ri386 version 4.0.5, an R-based bioinformatics platform used for gene intersection analysis, enrichment analysis and visualization. Venn diagrams were generated using Venny 2.1 to identify overlapping targets that may be involved in the antifibrotic activity of quercetin.

Protein–protein interaction (PPI) network construction

Protein–protein interaction analysis was conducted using the STRING database (version 11.0) (Szklarczyk *et al*., 2019). The species was limited to *Homo sapiens* and the minimum required interaction score was set to 0.7 (high confidence) to improve network reliability. The constructed PPI network was uploaded to Cytoscape 3.6.2 for topology analysis. The network parameters, including

Article in Press

degree centrality, clustering coefficient and average shortest path length, were calculated. Hub genes were identified using the cytoHubba plugin based on the Degree, Closeness and Betweenness algorithms (Yu *et al*., 2024).

Functional enrichment analysis

GO enrichment analyses, including biological process (BP), molecular function (MF) and cellular component (CC), as well as KEGG pathway analysis, were carried out using Ri386 4.0.5, DAVID 6.8, and Cytoscape (ClueGO plugin). Additional analyses were performed using R package DOSE, clusterProfiler and pathview. Visualization of enriched pathways related to quercetin and liver fibrosis was presented. Pathways with $p < 0.05$ were considered significant.

Liver fibrosis model, grouping and drug administration

After a 7-day acclimatization period, eighteen rats were randomly allocated to three groups (n = 6 per group): control group (CON), liver fibrosis model group (MOD) and quercetin treatment group (QR). Liver fibrosis was induced in the MOD and QR groups by subcutaneous injection of 40% carbon tetrachloride (CCl_4) dissolved in olive oil. An initial dose of 3 mL/kg was administered, followed by 5 mL/kg twice weekly for eight weeks, in accordance with previously reported protocols for the induction of experimental liver fibrosis. Quercetin (50 mg/kg/day) was administered to the QR group via oral gavage for eight weeks, starting on the first day of CCl_4 administration. The quercetin dose was chosen based on other publications reporting histopathological and biochemical improvements in liver injury/fibrosis in experimental models (50 mg/kg/day). However, quercetin has poor oral absorption, high first-pass metabolism and rapid biotransformation/pharmacokinetics, limiting overall exposure following oral administration. As such, higher doses often used in preclinical models may not translate to similarly higher exposures of the systemically available active drug but may instead offset low absorption/bioavailability rates. Doses do not always predict biologically relevant exposures. Therefore, the selected dose should be regarded as a preclinical investigative dose rather than a PK-optimized or clinically translatable dose. Saline solution of equal volume was administered via oral gavage to the CON and MOD groups throughout the study period. Body weight and overall health condition of animals were monitored weekly throughout the experiment. Twenty-four hours after last CCl_4 injection, rats were euthanized by intraperitoneal injection of sodium pentobarbital (150 mg/kg) and then liver tissues and cecal contents were collected. Liver tissues were used for histopathological assessments and cecal samples were frozen at −80°C until microbiota analysis.

Observation of general condition

Body condition was scored daily for rats throughout the experiment. This included mental status/activity, appearance of fur, consumption of food and change in body weight. Abnormal behaviors were noted.

Histopathological analysis of liver tissue

Liver tissues were fixed with 10% neutral buffered formalin, paraffin-embedded and sectioned at 3–4 μm thickness. Histological analysis was conducted with hematoxylin–eosin (H and E) staining and Masson's trichrome staining. H and E staining was performed with a commercially available staining kit (batch no. 20191231, Beijing Bio-Lab Technology Co., Ltd.). Masson staining was done using Masson's Trichrome Staining Solution (batch no. 20191025). Histological images were taken with an optical microscope (Olympus CX31) at 100× magnification. A total of at least five liver sections per rat were randomly selected and analyzed. Fibrosis was semi-quantitatively evaluated by using the Ishak scoring system (Kaya *et al*., 2025). Histopathological changes were blindly scored by two senior pathologists. Discrepancies were resolved by consensus after joint re-evaluation.

The Ishak scoring system evaluates fibrosis progression on a scale of 0–6:
0 — no fibrosis (normal liver)
1 — minimal fibrosis confined to the portal area
2 — portal fibrosis with expansion but without bridging
3 — septal fibrosis without bridging
4 — bridging fibrosis with preserved lobular structure
5 — bridging fibrosis with partial architectural distortion
6 — cirrhosis with pseudolobule formation and severe structural disruption

Cecal content collection and total bacterial DNA extraction

Immediately after euthanasia, each rat underwent aseptic exposure of the cecum, followed by sterile collection of cecal contents. All sampling procedures were performed using sterile equipment, including instruments and nuclease-free tubes and each animal was sampled separately to reduce contamination. Aliquots of approximately equal volume were collected from each rat's cecum contents. Immediately after sampling, all samples were snap-frozen in liquid nitrogen and stored at −80°C until DNA extraction (Triller *et al*., 2025).

DNA was extracted from cecal contents using the E.Z.N.A.® Stool DNA Kit (D4015, Omega Bio-tek, USA) following the manufacturer's instructions. A negative extraction control without a biological sample was included with each extraction to check for contamination from reagents or the environment. DNA quality and integrity were evaluated by 1% agarose gel electrophoresis. DNA concentrations were determined using UV spectrophotometer. The DNA samples that passed quality control were stored at −80°C for future 16S rRNA gene amplification and sequencing (Shin *et al*., 2026).

Article in Press

Amplicon sequencing of 16S rRNA

The composition of the bacterial community was analyzed by sequencing V3–V4 hypervariable regions of the 16S rRNA gene. PCR amplification was done with universal primers: 341F (5′-CCTACGGGNGGCWGCAG-3′) and 805R (5′-GACTACHVGGGTATCTAATCC-3′). PCR reactions were prepared in a 25 μL reaction system with 25 ng template DNA, 12.5 μL PCR premix, 2.5 μL of forward primer, 2.5 μL of reverse primer and nuclease-free water was added to adjust the final volume. PCR conditions were initial denaturation at 98 °C for 30 s, followed by 35 cycles of 98 °C for 10 s, 54 °C for 30 s and 72 °C for 45 s, with a final extension at 72 °C for 10 min. Each primer was tagged with unique barcode sequence and universal sequencing adapters at 5′ end to allow multiplex sequencing. PCR products were checked by electrophoresis on a 2% agarose gel. Amplicons with the target size were extracted from 2% agarose gel with AMPure XT magnetic beads (Beckman Colter Genomics, USA). The extracted PCR products were quantified using Qubit fluorometer (Invitrogen, USA) and fragment size distribution was analyzed with Agilent 2100 Bioanalyzer (Agilent Technologies, USA). A PCR negative control was added during the amplification steps to monitor for contamination. After quality control steps, PCR amplicons were used to construct sequencing libraries and sequenced on Illumina NovaSeq platform (PE250).

Sequencing data processing

Sequence data were processed using an established quality-control pipeline. Primer and adapter sequences were trimmed using Cutadapt (v1.9). Paired-end reads were assembled into paired reads using FLASH (v1.2.8) based on their overlapping sequences. Sequences were filtered by fqtrim (v0.94) for quality (reads were truncated if the average quality within a 100 bp sliding window was <20). Sequences shorter than 100 bp after trimming or assembling were removed and reads containing ambiguous bases (N) in more than 5% of positions were discarded.

Remaining high-quality sequences were analyzed using DADA2 (v2019.7), which incorporated denoising, error-correction algorithm and chimera removal to infer amplicon sequence variants (ASVs). Rarefaction analysis was performed to determine whether sufficient sequencing depth had been reached to capture the microbial diversity present in each sample. The resulting ASV table was used for subsequent analyses, including microbial diversity and community structure analysis. Although the average number of high-quality clean reads per sample was relatively modest (~1,240), rarefaction curves reached saturation and Good's coverage approached 1.0, indicating that the sequencing depth was sufficient to reliably characterize the dominant microbial taxa and overall community structure in this study. However, this depth may limit the confident detection of low-abundance rare taxa; therefore, findings related to rare taxa should be interpreted with caution. Future studies with deeper sequencing are recommended to further validate these observations.

Bioinformatics analysis

To minimize observer bias, histopathological scoring was performed independently by two senior pathologists in a blinded manner. For microbiome data, all processing, bioinformatics analysis and statistical testing were conducted using anonymized sample identifiers without knowledge of group allocation. Microbial community analyses were conducted using the ASV feature table and ASV representative sequences generated by DADA2. Before calculating alpha diversity indices, the ASV table was normalized to the minimum sequencing depth across all samples to reduce potential biases due to differences in sequencing depth.

Alpha diversity analysis

Alpha diversity indices were calculated using QIIME2 software (version 2019.7). Alpha diversity plots were constructed with R software. Rarefaction analysis was performed to assess whether the sequencing depth was sufficient to capture sample diversity.

Beta diversity analysis

Bray–Curtis dissimilarity distance was calculated to estimate beta diversity between groups. Non-metric multidimensional scaling (NMDS) was performed using Bray–Curtis dissimilarities to visualize differences in microbial communities among samples. Hierarchical clustering analysis based on Bray–Curtis dissimilarities was performed to evaluate the similarity of microbial communities between samples. Analyses were performed to determine differences in relative abundance between groups at each taxonomic level from phylum through genus. As many taxa were assessed concurrently, multiple comparisons were accounted for in downstream analyses to minimize false-positive results. Caution should be used when interpreting differential abundance findings of low-abundance taxa.

Differential taxa analysis

LEfSe analysis was performed on the OmicStudio platform (https: //www.omicstudio.cn/tool/60) to identify microbial taxa that differed significantly among groups. A statistical significance cutoff of $p < 0.05$ was set and linear discriminant analysis (LDA) scores of 2.0 were used to screen biomarkers.

Functional prediction analysis

PICRUSt2 software (version 2.2.0) was used to predict metagenomic functional profiles from 16S rRNA data. After predicting gene functions using the Clusters of Orthologous Groups (COG) database, Kyoto Encyclopedia of Genes and Genomes (KEGG) pathway annotations were assigned to the predicted COG-functional gene sets to identify potential functional pathways associated with differences in microbial communities between samples.

Article in Press

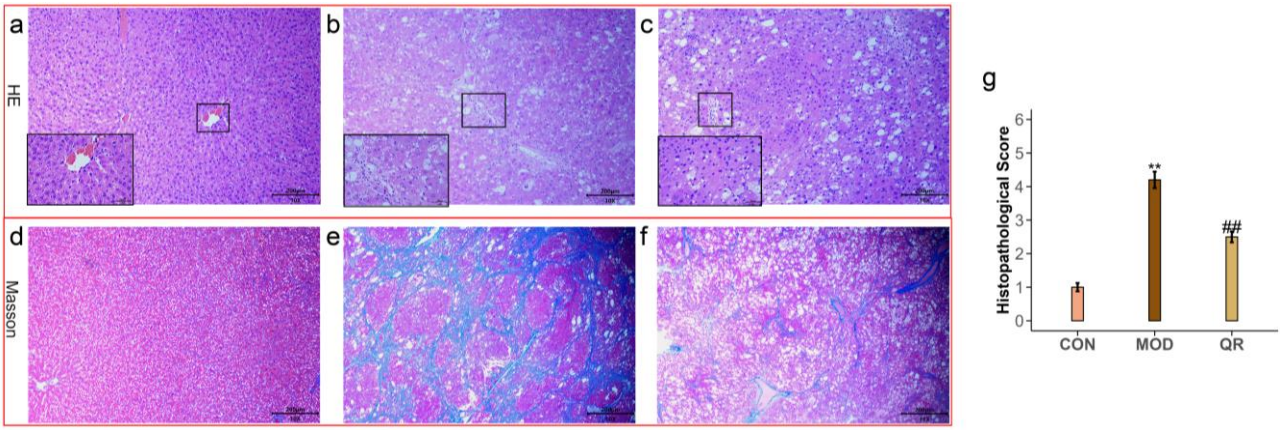


Fig. 1: Histopathological examination of rat liver tissue was conducted using hematoxylin and eosin (H and E) and Masson's Trichrome staining techniques. Panels (a, b and c) display H and E staining, while panels (d, e and f) exhibit Masson's Trichrome staining, all at 100× magnification. (a and d) Represent the control group (CON); (b and e) Illustrate the model group (MOD); (c and f) Depict the treatment group (QR); (g) Presents the histopathological scoring of liver tissue based on the Ishak score (vs. MOD group, ∗ ∗ $P < 0.01$; vs. QR group, ## $P < 0.01$).

Multiple tests were adjusted using the Benjamini–Hochberg FDR correction method and q-values < 0.05 were considered statistically significant.

Statistical analysis

All statistical analyses were conducted using IBM SPSS Statistics version 19.0 and R. Values are expressed as mean ± standard deviation (mean ± SD) unless otherwise stated. Prior to group comparisons, data distribution was examined for normality (Shapiro–Wilk test) and equality of variance (Levene's test). Differences between groups were analyzed using one-way analysis of variance (ANOVA) with Tukey's post hoc test for multiple comparisons when the data were normally distributed and the variances were equal among groups. When data failed normality tests, non-parametric tests were used (Kruskal–Wallis test). For microbiome data, statistical tests appropriate for comparing microbial abundance and diversity were conducted in QIIME2 and R. Adjusted p-values for multiple comparisons were estimated using the Benjamini–Hochberg method to control the false discovery rate (FDR). P <0.05 was considered statistically significant. Sample labels were anonymized during analysis/data processing/statistical testing as much as possible to reduce potential bias of group allocations. For microbiome-focused statistical tests comparing multiple taxa (such as Firmicutes and Bacteroidetes), p-values were adjusted for multiple comparisons (when possible) using Benjamini–Hochberg false discovery rate (FDR) correction. Corrected p-values, also referred to as q-values, were used to account for false discovery associated with type I error. A significant difference was accepted at a threshold of $q < 0.05$. For tests making pairwise/group comparisons in microbial relative abundance (i.e. Kruskal–Wallis), both uncorrected p-values and q-values were taken into account when considering results. LEfSe analysis uses the algorithm's built-in non-parametric testing with linear discriminant analysis (LDA) to determine statistical significance; thus, no p-values were extracted. LEfSe results were considered exploratory, as no consistent method for multiple-testing correction was available across all taxa. With this caveat in mind, microbiome-based statistics were interpreted with caution due to the high dimensionality of the data.

RESULTS

General condition of rats

Throughout the study, all rats in the three groups had access to both water and food. All rats in the CON group were shown to be mentally healthy and had no issues with their ability to eat or drink normally and had active movement and smooth coats as well as a steady increase in body weight. On the other hand, rats within the MOD group showed typical signs of liver fibrosis, such as loss of interest in eating, reduced water intake, slow movement, a rough coat, abdominal swelling and an overall bad mental state that peaked at 1-3 days after modeling was initiated. Rats in the QR group showed less severe clinical signs than those in the MOD group, with greater appetite, better activity, smoother coats, less body weight loss and an improved mental state.

Histopathological examination

Histopathological changes of liver tissue were evaluated by hematoxylin–eosin (H and E) staining and Masson's trichrome staining (Figs. 1a–1f). As shown in figure 1a, hepatic cords in CON group were neatly arranged. Hepatocytes showed normal morphology and little collagen fiber deposition was observed. Besides, there was no histological evidence of fibrosis. However, MOD group exhibited prominent pathological changes of liver fibrosis, including hepatocyte swelling, disorder of hepatic cords, focal necrosis, infiltration of inflammatory cells, thickened fibrous septa, extensive collagen deposition and formation of pseudo-lobules (Fig. 1b).

Article in Press

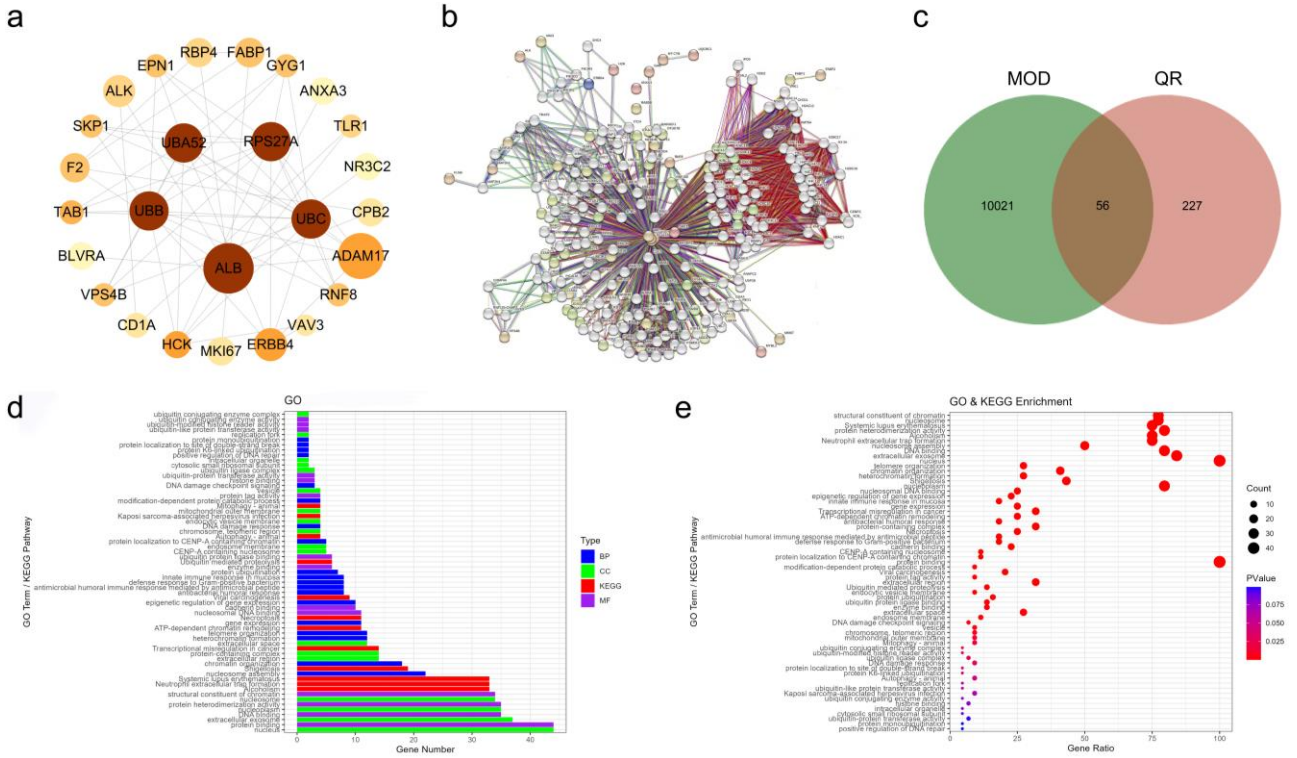


Fig. 2: Network pharmacology of quercetin in liver fibrosis. (a) Shared network of potential targets between quercetin and liver fibrosis; (b) Protein–protein interaction (PPI) network built by STRING database; (c) Venn diagram displaying the predicted targets of quercetin and liver fibrosis–related genes; (d) Gene Ontology (GO) analysis of overlapping targets divided into three categories: biological process (BP), molecular function (MF), and cellular component (CC); (e) KEGG pathway enrichment analysis of overlapping targets. Size of the bubble indicates the number of genes enriched in the pathway and color indicates the degree of statistical significance.

Compared with MOD group, liver tissues of QR group showed relatively mild histopathological changes, such as hepatocyte necrosis and inflammatory infiltration, fibrous septa were thinner and fewer pseudo-lobules and collagen deposition were observed (Fig. 1c). Similarly, the Ishak score of fibrosis was significantly increased in MOD group when compared with CON group ($P < 0.01$). Meanwhile, QR group had significantly lower fibrosis scores compared with MOD group ($P < 0.01$) (Fig. 1g). Taken together, these results indicate that quercetin administration was associated with reduced histopathological liver injury in CCl_4-induced liver fibrosis model.

Network pharmacology analysis

Target information of quercetin

Potential targets of quercetin were retrieved from literature studies and were also predicted using PharmMapper database. From this search, 310 candidate targets were retrieved. By eliminating duplicates and unifying the gene names based on UniProt database, 227 non-redundant targets were used for further analysis. In this network, proteins such as ALB and PKLR had relatively high degree values.

Identification of liver fibrosis-related targets and PPI network construction

Liver fibrosis–related genes were obtained from GeneCards and OMIM databases with "liver fibrosis" as the keyword. There were 10,361 disease genes collected from the databases, while 10,021 unique targets were acquired after deduplication. Venn analysis of quercetin targets and liver fibrosis–related genes revealed 56 intersections (Fig. 2), which were considered potential targets underlying quercetin's functions in liver fibrosis. Then these targets were uploaded into the STRING database to analyze the PPI network [species: Homo sapiens; minimum interaction score: 0.7 (high confidence)]. The interaction file was visualized using Cytoscape software, followed by further analysis of network topology parameters (degree, closeness centrality and betweenness centrality) using the CytoNCA plugin to screen out the key nodes. After screening the network based on network topology parameters (closeness $\geq$ 0.0322769, betweenness $\geq$ 280.98, degree $\geq 2 \times$ median), the core PPI network was obtained. Ultimately, 106 nodes with an average local clustering coefficient of 0.568 and PPI enrichment $p < 1.0 \times 10^{-16}$ were included in the final network (Figs. 2a and 2b).

Article in Press

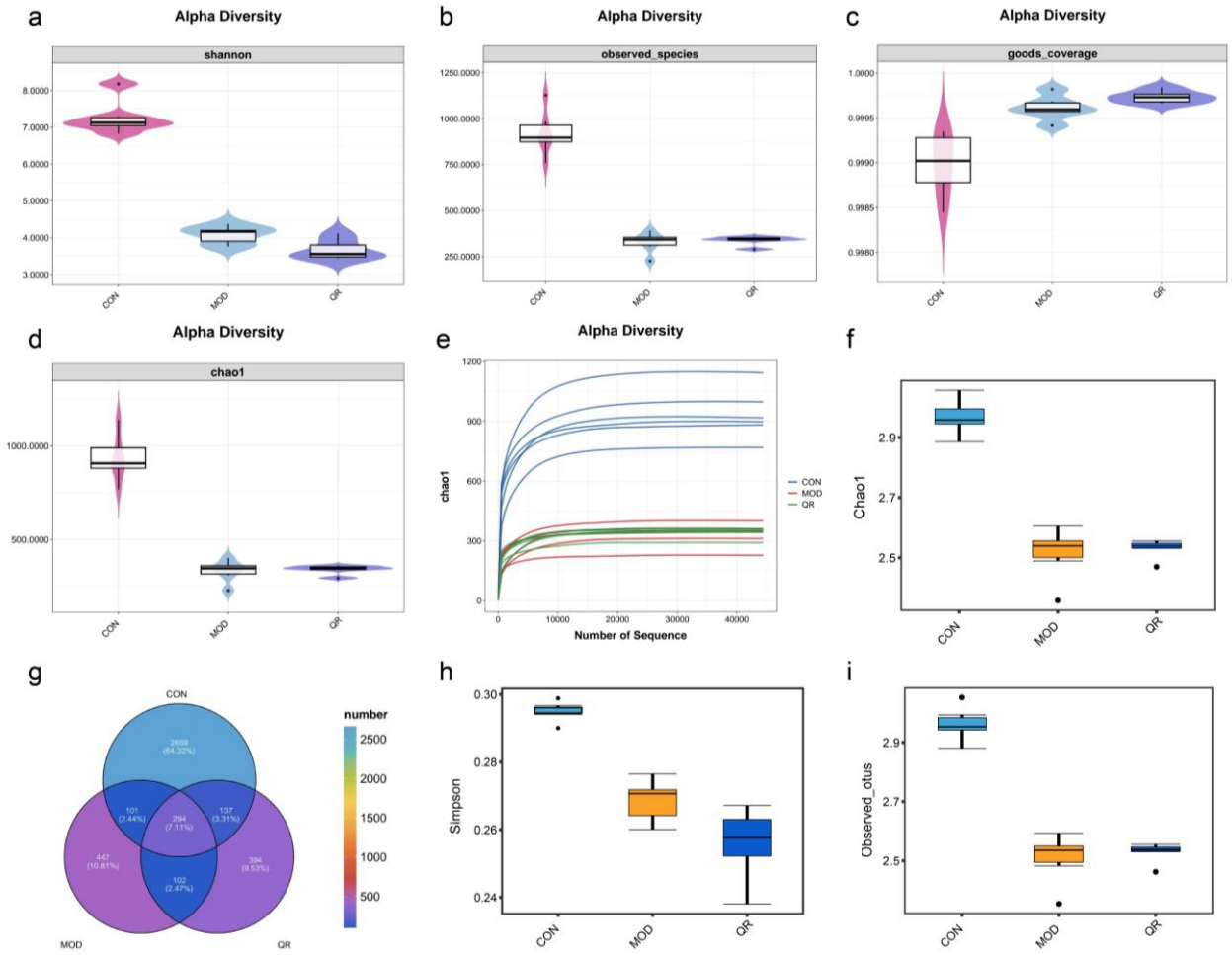


Fig. 3: Alpha diversity analysis and ASV distribution of gut microbiota among the experimental groups. (a) Shannon diversity index displayed microbial diversity of CON, MOD and QR groups; (b) Observed species index showed microbial richness of CON, MOD and QR groups; (c) Good's coverage index presented sequencing coverage across all samples; (d) Chao1 index was applied to estimate the species richness; (e) Chao1 rarefaction curve estimated sequencing depth versus species richness; (f) Box plot depicted values of Chao1 index among CON, MOD and QR groups; (g) Venn diagram illustrated shared and unique amplicon sequence variants (ASVs) among three groups; (h) Simpson diversity index demonstrated microbial diversity and evenness among CON, MOD and QR groups; (i) Number of observed ASVs among CON, MOD and QR groups.

GO functional annotation and KEGG pathway enrichment analysis

Functional enrichment analysis was performed on overlapping targets using R software and the DAVID database to identify potential biological functions and signaling pathways associated with quercetin targets in liver fibrosis. The top Gene Ontology (GO) terms enriched in CC, MF and BP categories are shown in figure 2d. The top enriched GO terms in CC included nucleosome, nucleoplasm, nucleus and extracellular exosome. The top enriched GO terms in MF included DNA binding, protein binding, histone binding and enzyme binding. The top enriched GO terms in BP included DNA damage response, chromatin organization and apoptosis. KEGG pathway analysis showed that 18 signaling pathways were potentially correlated with liver fibrosis (Fig. 2e). The top pathways, ranked by statistical significance and gene counts, included the TNF signaling pathway, p53 signaling pathway, HIF-1 signaling pathway, Toll-like receptor signaling pathway, nucleotide metabolism, and ubiquitin-mediated proteolysis. Overall, quercetin-related targets were enriched in multiple biological processes and signaling pathways related to liver fibrosis. It is worth mentioning that these analyses were based on database prediction and enrichment and their biological functions require further experimental validation.

Impact of quercetin intervention on gut microbiota diversity in rats with liver fibrosis

Analysis of quercetin's influence on gut microbiota diversity in liver fibrosis

Cecal content samples from the CON, MOD and QR groups (six samples each) were subjected to cecal content analysis.

Article

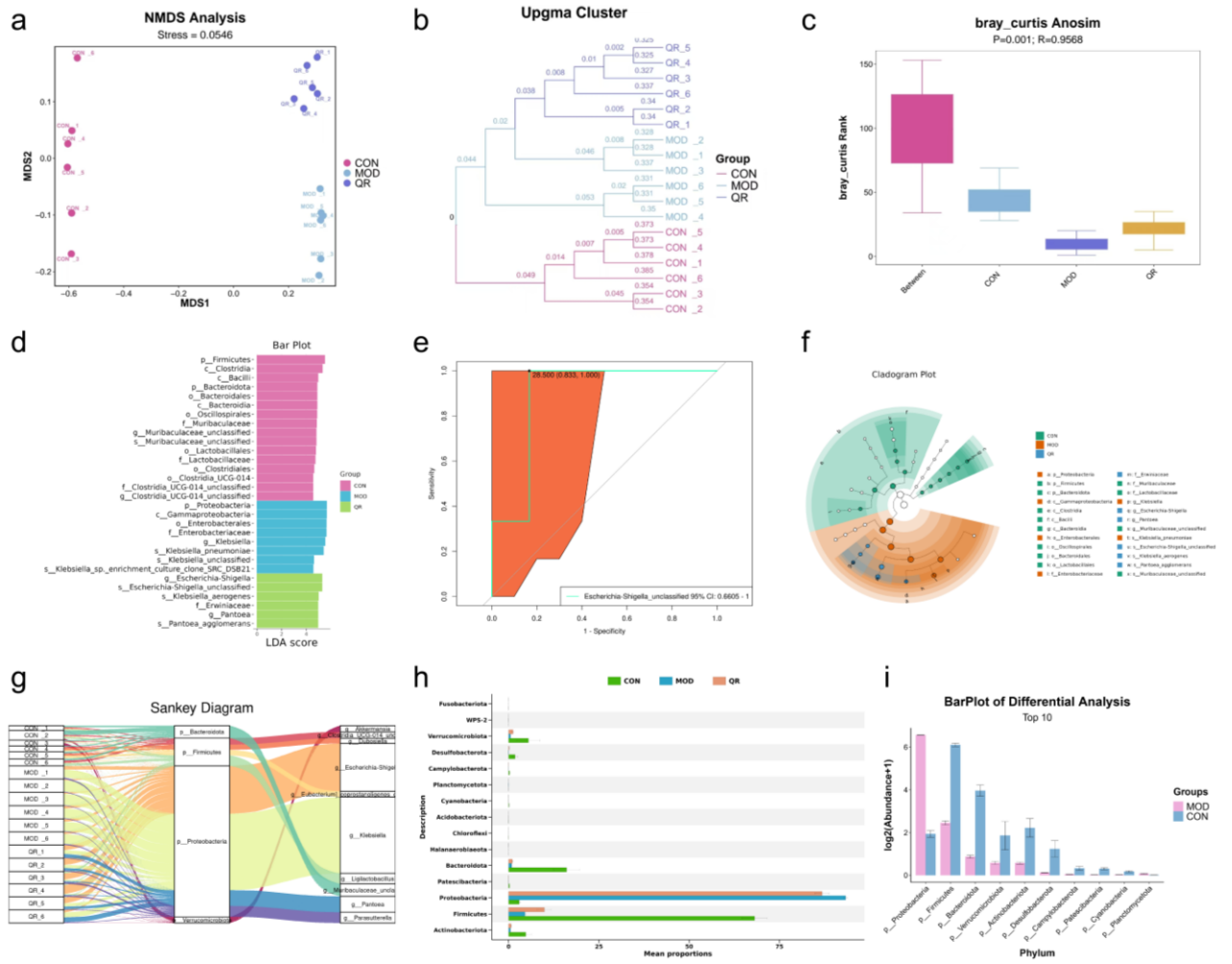


Fig. 4: The analysis of beta diversity and differential microbiota composition in rats with liver fibrosis undergoing quercetin intervention.

(a) Non-metric multidimensional scaling (NMDS) plot based on Bray–Curtis distance among samples from CON, MOD, and QR groups. Each dot represents an individual sample; (b) Unweighted pair group method with arithmetic mean (UPGMA) cluster analysis based on Bray–Curtis distance; (c) Analysis of similarities (ANOSIM) based on Bray–Curtis distance among groups; (d) Linear discriminant analysis (LDA) score bar plot of taxa showing differential abundance among groups; (e) Receiver operating characteristic (ROC) curve of *Escherichia–Shigella*; (f) LEfSe cladogram presenting taxa showing differential abundance among groups. The depth of the branch indicates the taxonomic level; (g) Sankey diagram showing the relative abundance of microbial taxa at the phylum to genus level; (h) Bar plot showing relative abundance of microbial taxa at the phylum level; (i) Differential abundance of microbial taxa at the phylum level.

The composition of the microbial community was determined by sequencing of V3–V4 variable region of 16S rRNA gene. A total of 22,321 raw sequences were obtained after quality filtering and removal of chimeric sequences with VSEARCH (version 2.3.4), yielding an average of 1,240 clean reads per sample. The analysis showed that about 99.89% of sequences belonged to the V3–V4 region of the 16S rRNA gene and fragment lengths were between 400 and 500 bp, suggesting that the targeted region was indeed the V3–V4 region. Quantitative Insights into Microbial Ecology 2 (QIIME2) was used to generate amplicon sequence variants (ASVs). The number of ASVs shared and not shared among the three groups is shown in figure 3 as a Venn diagram. A total of 12,770 ASVs were obtained among all samples. There were 431 ASVs that were shared between QR and CON groups and 396 ASVs were shared between QR and MOD groups.

The numbers of unique ASVs observed for the CON, MOD and QR groups were 2,659, 447 and 394, respectively. The MOD group had the highest number of total ASVs among the three groups. The QR group had fewer ASVs than the other groups.

Article

Alpha diversity analysis

Alpha diversity analysis was performed to estimate microbial richness and diversity in each sample. Microbial diversity was estimated by calculating the Shannon–Wiener index. Rarefaction curves were constructed to analyze sequencing coverage depth. Shannon index values for all samples ranged from 7 to 9 (Fig. 3a). These results suggest that the sequencing depth captured the major features of microbial diversity; however, detection of low-abundance taxa may be limited. Several alpha diversity indices were compared among groups, including Observed_species, Chao1, Simpson index and Shannon index (Figs. 3b–3i). The MOD group had significantly higher Observed_species, Chao1, Simpson and Shannon indices than the other two groups ($P < 0.05$). Good's coverage of all samples was close to 1.

Beta diversity analysis

Beta diversity among three experimental groups was then examined. NMDS based on Bray–Curtis dissimilarities clearly separated the samples from the CON and MOD groups (Fig. 4a). QR samples clustered closer to the MOD samples. Moreover, UPGMA hierarchical clustering analysis also showed a similar pattern (Fig. 4b). CON samples formed their own cluster and MOD and QR samples were closer to each other. Differences in microbial community structure among the three groups were further examined by analysis of similarities (ANOSIM) using the Bray–Curtis distance matrix as the similarity coefficient. A significant difference was observed among the three groups ($P = 0.001$, $R = 0.9568$) (Fig. 4c) and the between-group variability was larger than the within-group variability.

LEfSe analysis

Linear discriminant analysis effect size (LEfSe) analysis revealed taxa that were differentially abundant among the CON, MOD and QR groups (Figs. 4). Firmicutes, Clostridia, *Muribaculaceae* and *Lactobacillaceae* were found to be relatively enriched in CON rats. While Proteobacteria, *Klebsiella* and *Escherichia–Shigella* were enriched in MOD rats. QR rats showed an increase in the relative abundance of *Pantoea agglomerans* and the *Erwiniaceae*. Receiver operating characteristic (ROC) curve analysis revealed *Escherichia–Shigella* may potentially be used as a microbial biomarker associated with liver fibrosis. (Sensitivity = 0.833, specificity = 1.000 and area under the curve ranged from 0.6605–1) (Fig. 4e). The LEfSe cladogram is displayed in figure 4f. Taken together, these results demonstrate that certain microbial taxa differed between groups.

Sample and species distribution analysis

The Sankey diagram (Fig. 4g) represented microbial community compositions of samples at the phylum and genus levels. MOD group had higher relative abundance of Proteobacteria and Bacteroidota phyla, which comprised *Escherichia–Shigella, Eubacterium coprostanoligenes* group and *Klebsiella* genera among others. The CON group had a higher relative abundance of the phylum Firmicutes and the genera Clostridia UCG-014 and Dubosiella within other phyla than the MOD group. QR group exhibited lower relative abundance of *Klebsiella* and higher relative abundance of *Muribaculaceae*, *Ligilactobacillus* and *Pantoea* compared with MOD group. The results of STAMP analysis were shown in the figure. 4h. Through differential abundance analysis (Fig. 4i) at the phylum level, it was shown that the MOD group had higher relative abundances of the Proteobacteria and Actinobacteriota phyla and lower relative abundance of Firmicutes compared with the CON and QR groups.

Analysis of gut microbiota composition and structure in different groups

The relative abundance of bacterial taxa at the phylum level of the three groups is depicted in figure 5a. Proteobacteria, Firmicutes, Bacteroidota, Actinobacteriota and Verrucomicrobiota were the predominant phyla in all samples. MOD exhibited a higher relative abundance of Proteobacteria and lower relative abundance of Firmicutes compared with CON. Firmicutes was one of the most dominant microbiota members in CON (Fig. 5b). QR had a lower relative abundance of Proteobacteria than MOD and a higher relative abundance of Firmicutes (Fig. 5b). At the class level, the differences in microbial composition among groups are shown in figure 5c. MOD had a higher relative abundance of Gammaproteobacteria and Bacteroidia and a lower relative abundance of Clostridia and Bacilli compared with CON ($P < 0.05$). The QR group exhibited microbial compositions that differed from those of MOD (Fig. 5d). Results of the hierarchical clustering analysis also showed differences in microbial community composition among the three groups (Fig. 5e). MOD had a higher relative abundance of Gammaproteobacteria and lower relative abundance of Clostridia and Bacilli compared with CON. QR showed differences from MOD and similarities to CON for certain taxa (Fig. 5f).

Correspondence analysis of gut microbiota distribution

The Circos plot (Fig. 5g) showed the distribution of gut microbes at different taxonomic levels (>genus) among samples. Gut microbiota composition varied among the CON, MOD and QR groups. Compared with CON group, MOD group had relatively increased abundance of Proteobacteriales, Enterobacterales and Bacteroidales orders, whereas Clostridiales and Lactobacillales orders had lower relative abundance. Clostridiales and Lactobacillales were predominant members of the gut microbiota in the CON group, while the gut microbiota in the MOD group had relatively higher abundance of Pseudomonadales and Enterobacterales orders. The QR group had a different microbial composition from the MOD group and, in several taxa, similar abundance levels to the CON group. This observation was consistent with the abundance distributions of microbial taxa at the phylum level (Figs. 5a and 5b).

Article in Press

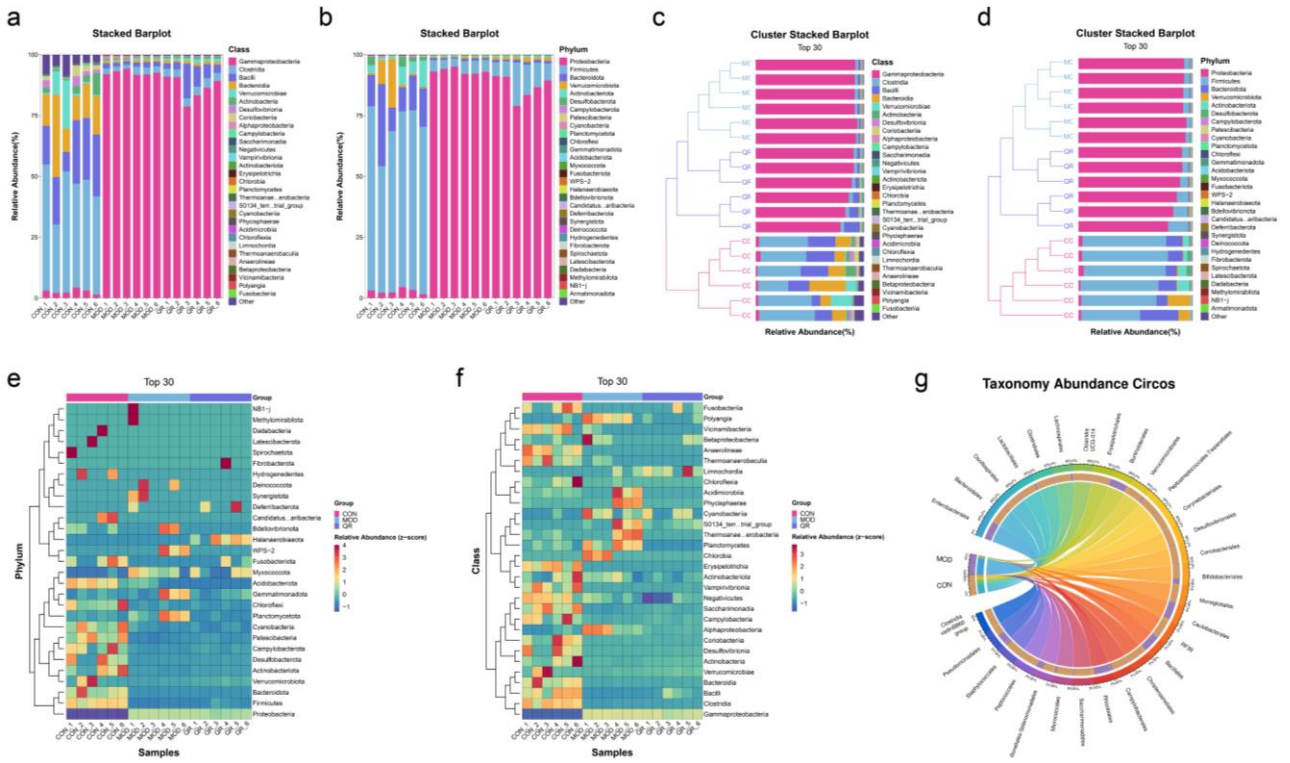


Fig. 5: Gut microbiota composition and taxonomic distribution across experimental groups. (a) Relative abundance of microbial taxa at phylum level among CON, MOD and QR groups were presented as stacked bar plot; (b) Relative abundance of microbial taxa at class level among groups were presented as stacked bar plot; (c) Distribution of microbial taxa at class level among samples were displayed as clustered stacked bar plot; (d) Distribution of microbial taxa at phylum level among groups were displayed as clustered stacked bar plot; (e) Heatmap representation of microbial abundance difference and clustering at phylum level; (f) Heatmap representation of microbial composition difference and clustering at class level; (g) Circos plot presentation of microbial taxa distribution at order level among groups.

Functional prediction analysis

To predict the functional potential of the gut microbiota, PICRUSt2 was used to infer metabolic functions from 16S rRNA sequencing data by comparing ASVs against annotated reference genomes in the KEGG database. Functional profiles were assessed at the level of KEGG pathway annotations and Enzyme Commission (EC) categories. PICRUSt2 analysis at the KEGG pathway level (Figs. 6a and 6b) showed altered predicted functional modules between MOD and CON groups. Compared to CON group, MOD rats displayed higher predicted abundance of functional pathways related to carbohydrate metabolism, lipopolysaccharide (LPS) biosynthesis, nucleotide repair and DNA replication. Predicted functional capacities associated with signal transduction, protein translation and nervous system were relatively decreased.

KEGG level 3 analysis (Fig. 6b) revealed higher predicted representation of LPS biosynthesis pathways, DNA replication proteins, amino sugar and nucleotide sugar metabolism, D-alanine metabolism, glycine, serine and threonine metabolism, galactose metabolism and purine metabolism in MOD rats. Predicted functions associated with nucleotide repair mechanisms such as nucleotide excision repair and DNA polymerases were higher in MOD rats compared to CON rats.

PICRUSt2 analysis at the EC level (Figs. 6c and 6d) showed higher predicted enzyme categories associated with nucleotide metabolism, lipid metabolism and carbohydrate metabolism in MOD rats. Predicted enzymes associated with pathways discussed above, including those involved in LPS biosynthesis, nucleotide reductases and gluconeogenesis-related enzymes, were higher in MOD rats compared to CON rats. PICRUSt2 analysis at the KO level showed higher representation of genes associated with iron metabolism and LPS biosynthesis (Fig. 6e). In addition, predicted genes encoding transporter proteins and membrane-binding proteins were higher in MOD rats.

Metabolic pathway comparison between CON and MOD rats (Fig. 6f) revealed several pathways with higher representation in MOD rats compared to CON rats, including D-galacturonate I degradation, sucrose degradation IV (sucrose phosphorylase pathway), degradation of purine bases I (anaerobic) and lipopolysaccharide synthesis.

Article in Press

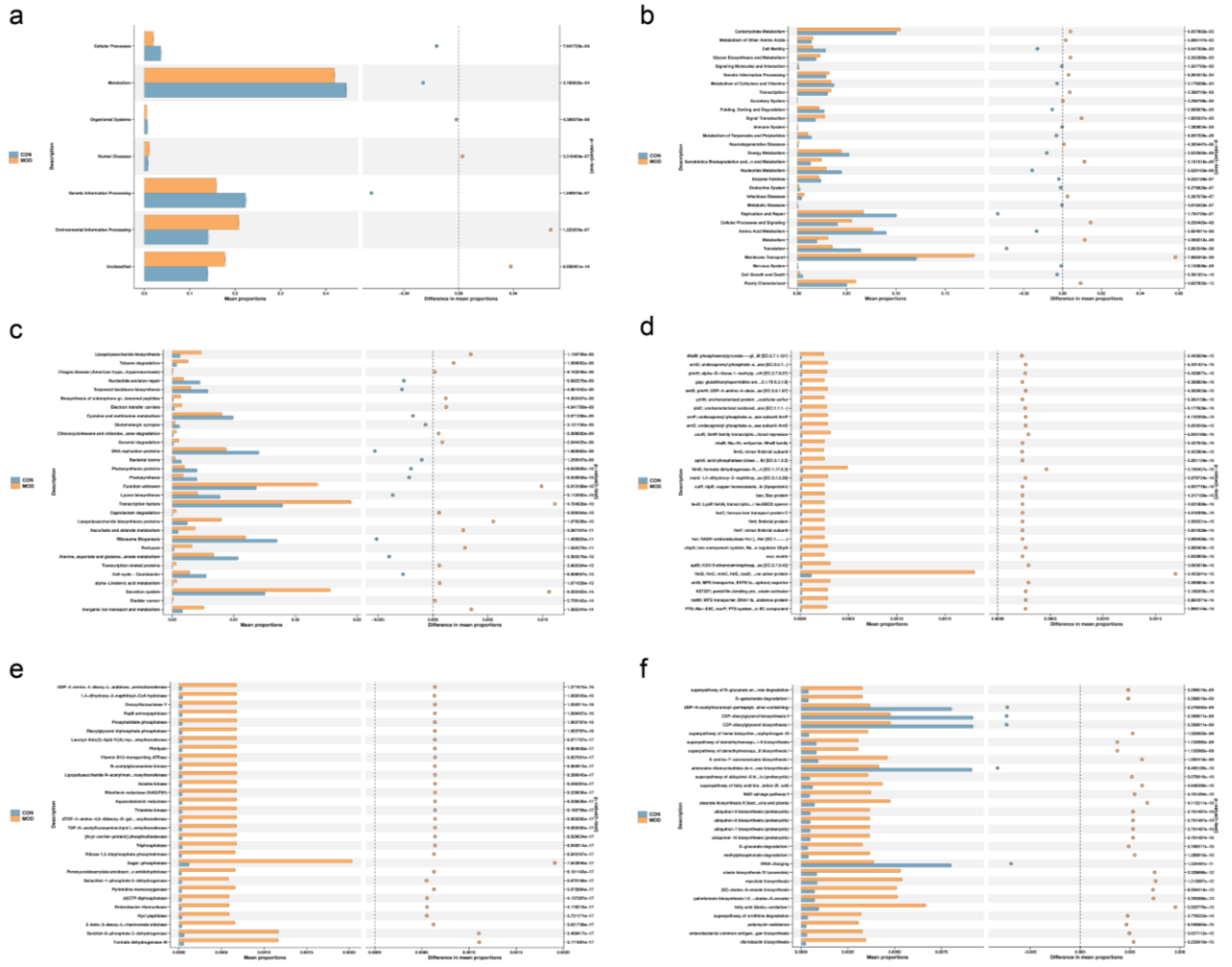


Fig. 6: Predicted functional profiles of gut microbiota based on PICRUSt2 analysis. (a) Predicted functional pathways based on Kyoto Encyclopedia of Genes and Genomes (KEGG) annotations from the CON group and MOD group analyzed using LEfSe; (b) Predicted KEGG functional categories from all samples visualized as a bar plot; (c) Predicted Cluster of Orthologous Groups (COG) functional categories from all experimental groups visualized as a bar plot; (d) Predicted abundance of gene families within the microbial communities visualized as a bar plot; (e) Predicted enzyme categories based on enzyme commission (EC) numbers visualized as a bar plot; (f) Predicted functional genes from all microbial communities visualized as a bar plot.

Predicted metabolic pathways with lower representation in MOD rats included ubiquinone biosynthesis, beta-oxidation of fatty acids, phenylalanine metabolism, valine, leucine and isoleucine metabolism, and glyoxylate and dicarboxylate metabolism.

DISCUSSION

Histopathological alterations, gut microbiota structure and predicted microbial functional profiles after treatment with quercetin were investigated using a rat model of liver fibrosis induced by CCl_4. Injury induced by CCl_4 has been used extensively in preclinical studies because it recapitulates many aspects of hepatic fibrogenesis such as hepatocyte damage, infiltration of inflammatory cells, deposition of extracellular matrix proteins and formation of fibrous septa (Zhang *et al*., 2020). Evaluation of liver injury and fibrosis using H and E staining, Masson staining and Ishak scoring revealed that liver injury and fibrosis were exacerbated in the MOD group compared to QR group. These results were generally consistent with previous studies and indicated that structural changes in the liver were milder after quercetin treatment in this model of liver fibrosis. However, there are several limitations to note when considering this model. First, while there are histological similarities between CCl_4-induced liver injury and human liver fibrosis, chronic liver diseases in humans can be caused by several mechanisms such as viral hepatitis, metabolic dysfunction–associated steatotic liver disease, alcohol-related liver disease, cholestatic liver disease and autoimmune liver injury (Cheemerla *et al*., 2021). Pathogenesis between these diseases can vary in

immune cell infiltration, clinical course and gut microbial changes (Shim *et al*., 2023). Second, there are inherent differences in microbiota composition and ecology between rodents and humans (Liu *et al*., 2022). Therefore, translation of these results to humans should be done with caution.

Growing evidence suggests that gut microbial dysbiosis may drive liver fibrosis through alterations in the gut–liver axis (Siddle *et al*., 2026). Efforts have been made to determine how microbial components (cell walls, membranes, nucleic acids), metabolites and immune-related mediators access the portal circulation and modulate hepatic inflammation and fibrogenesis (Ronca *et al*., 2025). Gut microbiota composition significantly differed between the CON and MOD groups, consistent with prior reports that microbial community composition is altered during liver fibrosis. Alpha-diversity and beta-diversity analyses both showed separation by group; however, these are associative findings and cannot determine whether alterations in the microbiota are drivers of disease progression, consequences of disease progression or occur concurrently with other changes.

Interestingly, alpha diversity was increased in MOD animals relative to CON animals based on Observed species, Chao1, Simpson and Shannon indices. This contrasts with previous reports. Studies in other liver injury models have reported similar increases. Some studies, however, particularly those using models of more severe/advanced disease, have reported decreases in alpha diversity or no obvious change. Such variation may be attributed to species differences, experimental design, severity/duration of liver insult, intestinal sampling site, sequencing depth, etc., as well as differences in bioinformatic pipelines. This may reflect differences in temporality, specifically that during certain stages of dysbiosis, an expansion of many taxa may increase observed diversity, whereas at other stages, the continued accumulation of damage results in microbial community collapse and a loss of diversity. Irrespective of causality, increased alpha diversity as observed in this study is not inherently positive or negative.

A similar pattern was found in beta-diversity analyses. Both NMDS and UPGMA clustering revealed clear discrimination between CON and MOD groups, while ANOSIM indicated between-group differences in overall microbial community structure. Notably, the QR group clustered closer to the MOD group than to the CON group. These results suggest that under the experimental conditions employed here, treatment with quercetin led to detectable alteration of microbial community structure but failed to reinstate an overall control-like community pattern. That is, the microbiota alteration in the QR group appeared partial rather than complete. At the taxonomic level, several differences between groups were noted. As expected, the MOD group was characterized by increased relative abundance of Proteobacteria and decreased relative abundance of Firmicutes, together with enrichment of Escherichia–Shigella, Klebsiella and other taxa. These taxonomic shifts have been noted in other models of liver injury and microbial dysbiosis. By contrast, the CON group was enriched in Firmicutes-associated taxa such as Clostridia and Lactobacillales, while the QR group exhibited intermediate abundance of these taxa. Taken together, these data suggest that treatment with quercetin was associated with a partial alteration in gut microbiota composition under the conditions examined here. However, because microbial function was not directly assessed here, it is not possible to definitively categorize the identified taxa as beneficial or harmful. The functional impact of specific taxa is likely context-dependent and may vary with host condition and microbial ecology. LEfSe analysis identified additional taxa with differential abundance among groups. As noted above, *Escherichia–Shigella* was enriched in the MOD group. Members of this genus have been linked to intestinal dysfunction and inflammatory disorders in other models. However, despite this precedent, the finding reported here should be interpreted with caution; it merely represents a taxonomic association rather than definitive evidence that this genus mechanistically contributes to fibrosis development. The same level of caution should be applied to taxa identified by ROC analysis as having putative discriminatory capacity. Given the small sample size and the exploratory nature of the microbiome analysis, all such observations should be considered preliminary.

Another unique aspect of the present study was the combination of network pharmacology with microbiota analysis. Network analysis revealed hub targets (UBC, UBE2I, RBX1, PSMB7, UBA1) and enriched pathways including TNF signaling, p53 signaling, Toll-like receptor signaling, HIF-1 signaling and ubiquitin-mediated proteolysis. Hub targets and enriched pathways were generally implicated in protein turnover, stress response, inflammatory regulation and tissue remodeling which have been implicated in liver fibrosis throughout the above discussion. Considering these findings together, network analysis from the present study allows us to contemplate possible overlaps between quercetin-associated target prediction and biological processes associated with hepatic injury and/or host–microbiota relationships. It is important to note that these target–pathway relationships were inferred using bioinformatic prediction methods and were not experimentally validated. As such, they should be considered hypothesis-generating and not mechanistic evidence.

This is another important consideration when implicating mechanisms discussed in the above literature. The relationship between microbiota alterations and liver fibrosis has been hypothesized to be connected through bile

Article in Press

acid metabolism, lipopolysaccharide translocation, short-chain fatty acid signaling and immune cell trafficking. However, these parameters were not measured or analyzed in the present study. There were no measurements of SCFAs, bile acids, inflammatory cytokines, or immune cell populations. As such, although discussed, the taxonomic alterations cannot be directly linked to these mechanisms of action. The current dataset only allows us to speculate on these literature-derived mechanisms as possible explanations.

Likewise, PICRUSt2 analysis predicted differences in microbial functional potential related to carbohydrate metabolism, lipopolysaccharide biosynthesis, nucleotide repair and DNA replication between MOD and CON groups. Altogether, these data may suggest that liver fibrosis in the model was associated not only with changes in microbiota composition, but also with alterations in predicted microbial functional potential. However, PICRUSt2 analysis does not directly measure gene expression, enzyme activity or metabolite production. PICRUSt2 analysis predicts functional potential based on gene content of reference genomes. As such, these results are also considered hypothesis-generating rather than confirmatory of changes in microbial metabolism.

Limitations of study include small sample size, use of male rats only with no assessment of sex-specific differences, cross-sectional analysis of microbiota composition during fibrosis development and quercetin treatment, lack of molecular validation of predicted mechanisms despite blinded histopathology, potential cage effects due to use of co-housed animals as in many microbiome investigations and relatively shallow sequencing that could limit detection of low-abundance taxa and interpretation of diversity and differential abundance analyses. While rarefaction indicated good sampling of dominant taxa, the relatively shallow sequencing depth may have limited the ability to detect taxa at low abundances, ultimately reducing the detection of total microbial diversity. However, major differences in community structure or at higher taxonomic levels were unlikely to have been missed. Dominant taxa should not be substantially affected by the relatively low number of sequences obtained.

Limitations of the network pharmacology analysis itself include those inherent in the prediction algorithms and databases on which it is built. Future studies are warranted that include larger sample sizes, increased sequencing depth, longitudinal sampling and validation at the molecular or metabolite level.

CONCLUSION

Briefly, the study explored the relationships between quercetin intervention, liver fibrosis and gut microbiota by histopathological examination, network pharmacology prediction and 16S rRNA gene sequencing based on CCl_4 - induced rat model of liver fibrosis. Liver fibrosis is associated with severe histological damage and gut microbiota dysbiosis. Quercetin intervention is associated with milder histopathological changes and shifts in microbiota composition. Meanwhile, network pharmacology prediction and microbiota profiling found potential targets/pathways and microbiota alterations, respectively. There are still correlations/partial predictions above that need further study with larger sample sizes from both genders and repeated microbiome sequencing before and after the intervention.

Acknowledgments

In accordance with the recommendations from the International Committee of Medical Journal Editors (ICMJE) and the Committee on Publication Ethics (COPE), as also indicated in the instructions for authors of the journal, authors are expected to transparently disclose the use of AI tools. Accordingly, the assistance of the AI tool ChatGPT (developed by OpenAI, San Francisco, USA) is acknowledged for language editing and polishing of the manuscript. The tool was used solely for improving clarity, grammar and fluency in expression. No AI was employed for generating scientific ideas, data analysis, interpretation, figure preparation, or image creation. All academic content, including hypotheses, interpretation of results, and conclusions, was independently developed and verified by the authors. The authors take full responsibility for the integrity, originality and accuracy of the manuscript.

Author's contributions

Ruiqi Zhao and Feng Bai: Conceptualization, visualization and drafting of the manuscript; Bingxuan Fan, Shufang Niu and Peng Wang: Data curation and writing of the original draft; Wanfu Bai, Mingkai Qin and Donghua Zheng: Funding acquisition, supervision, manuscript review and editing; Jianfang Sun, Jiali Liu, Jun Qi and Xiaowen Song: Contributed through methodology development, investigation, validation and resource acquisition. All the authors read and approved the published version of the manuscript.

Funding

This study received financial support from multiple research funding sources, including the National Natural Science Foundation of China (82460834), the Natural Science Foundation of Inner Mongolia Autonomous Region, China (2024MS08025, 2024QN08090, 2025LHMS08049), the Baotou Health Science and Technology Program (2024wsjkkj70). Additional support was provided by the Inner Mongolia Autonomous Region Graduate Research and Innovation Project (KC2025079S), the Pharmacy Quality Improvement and Cultivation Discipline Construction Project of Baotou Medical College (YXTZ202606, YXTZ202607, YXTZ202610), the 2025

Article in Press

"Bud Plan" Project of Baotou Medical College (HLJH202508, HLJH202607, HLJH202622, HLJH202628), the Science and Technology Program of the Joint Fund for Scientific Research in Public Hospitals under Inner Mongolia Academy of Medical Sciences (2023GLLH0183, 2024GLLH0529), the College Student Innovation and Entrepreneurship Training Program (S202510130003, S202610130013) and the Scientific Research Development Fund Project of Baotou Medical College (BYJJ-GCJH202602).

Data availability statement

The datasets used and/or analyzed during the current study are available from the corresponding author upon reasonable request.

Ethical approval

This study was approved by the Baotou Medical College Animal Ethics Committee (Approval No. 2022-961). This study was performed in adherence with the ARRIVE guidelines. See supplementary file for the ARRIVE checklist.

Conflict of interest

The authors declare no conflict of interest.

REFERENCES

Barazesh M, Malekpour M, Akhzari M, Abouali B and Soltaninejad M (2026). Latest updates on pharmaceutical properties of quercetin and its derivatives as bioactive flavonoids in health protection and disease treatment. *Curr. Drug Ther.*, in press.

Cheemerla S and Balakrishnan M (2021). Global epidemiology of chronic liver disease. *Clin. Liver Dis.*, **17**(5): 365-370.

Chen P, Zou F and Liu W (2025). Recent advancement in prevention against hepatotoxicity, molecular mechanisms, and bioavailability of gallic acid, a natural phenolic compound: Challenges and perspectives. *Front. Pharmacol.*, **16**: 1549526.

Feuermann M, Mi H, Gaudet P, Muruganujan A, Lewis SE, Ebert D, Mushayahama T, Gene Ontology Consortium and Thomas PD (2025). A compendium of human gene functions derived from evolutionary modelling. *Nature*, **640**(8057): 146-154.

GeneCards (2025). GeneCards: The Human Gene Database. Available at: https://www.genecards.org/ (Accessed 5 September 2025).

He R, Qi P, Shu L, Ding Y, Zeng P, Wen G, Xiong Y and Deng H (2025). Dysbiosis and extraintestinal cancers. *J. Exp. Clin. Cancer Res.*, **44**(1): 44.

Kaya E, Simsek H, Ulucan A and Dortbudak MB (2025). Natural shield against arsenic threat: Potential of royal jelly to protect rat liver against sodium arsenite toxicity. *Environ. Sci. Pollut. Res.*, **32**(38): 22403-22416.

Kim S, Chen J, Cheng T, Gindulyte A, He J, He S, Li Q, Shoemaker BA, Thiessen PA, Yu B, Zaslavsky L, Zhang J and Bolton EE (2023). PubChem 2023 update. *Nucleic Acids Res.*, **51**(D1): D1373-D1380.

Li X, Li S and Li N (2025). Research progress on natural products alleviating liver inflammation and fibrosis via NF-κB pathway. *Chem. Biodivers.*, **22**(4): e202402248.

Li X, Yang S, Zhu L, Song H, Lin L and Cao C (2025). Protective effects of quercetin on LPS-induced liver injury in quails. *Toxicon*, **265**: 108496.

Liu H, Liao C, Wu L, Tang J, Chen J, Lei C, Zheng L, Zhang C, Liu YY, Xavier J and Dai L (2022). Ecological dynamics of the gut microbiome in response to dietary fiber. *ISME J.*, **16**(8): 2040-2055.

Liu X, Liang Q, Qin Y, Chen Z and Yue R (2025). Advances and perspectives on the anti-fibrotic mechanisms of the quercetin. *Am. J. Chin. Med.*, **53**(5): 1411-1440.

Online Mendelian Inheritance in Man (OMIM) (2025). Online Mendelian Inheritance in Man. Available at: https://omim.org/ (Accessed 5 September 2025).

Qiang R, Zhang Y and Wang Y (2022). Mechanisms of Xiaochaihu decoction on treating hepatic fibrosis explored by network pharmacology. *Dis. Markers*, **2022**: 8925637.

Ronca V, Gerussi A, Collins P, Parente A, Oo YH and Invernizzi P (2025). The liver as a central "hub" of the immune system: Pathophysiological implications. *Physiol. Rev.*, **105**(2): 493-539.

Ru J, Li P, Wang J, Zhou W, Li B, Huang C, Li P, Guo Z, Tao W, Yang Y, Xu X, Li Y, Wang Y and Yang L (2014). TCMSP: A database of systems pharmacology for drug discovery from herbal medicines. *J. Cheminform.*, **6**: 13.

Shen Y, Fan N, Ma SX, Cheng X, Yang X and Wang G (2025). Gut microbiota dysbiosis: Pathogenesis, diseases, prevention and therapy. *MedComm*, **6**(5): e70168.

Shim JA, Ryu JH, Jo Y and Hong C (2023). The role of gut microbiota in T cell immunity and immune mediated disorders. *Int. J. Biol. Sci.*, **19**(4): 1178-1191.

Shin S and Lee Y (2026). Quantitative polymerase chain reaction-based UV biodosimetry using indigenous 16S rRNA genes enables dose-verified validation of wastewater disinfection reactors. *ACS ES&T Water*, **6**(4): 2522-2532.

Siddle M, Gallego Duran R, Goel D, Renquist BJ, Holt MK and Hadjihambi A (2026). Mechanistic insights into the liver-brain axis during chronic liver disease. *Nat. Rev. Gastroenterol. Hepatol.*, **23**(2): 166-188.

Szklarczyk D, Gable AL, Lyon D, Junge A, Wyder S, Huerta-Cepas J, Simonovic M, Doncheva NT, Morris JH, Bork P, Jensen LJ and von Mering C (2019). STRING v11: Protein-protein association networks with increased coverage, supporting functional discovery in genome-wide experimental datasets. *Nucleic Acids Res.*, **47**(D1): D607-D613.

Article in Press

Triller S, Beasy G, Hughes S, Serghiou I and Ahn-Jarvis J (2026). Collection, storing, and processing of other samples. In: Carding SR (ed.), *Best Practice in Microbiome Research*. Humana, New York, NY, pp. 45-59.

UniProt Consortium (2025). UniProt. Available at: https://www.uniprot.org/ (Accessed 5 September 2025).

Venny (2025). Venny 2.1: An interactive tool for comparing lists with Venn diagrams. Available at: https://bioinfogp.cnb.csic.es/tools/venny/index.html (Accessed 5 September 2025).

Wang X, Shen Y, Wang S, Li S, Zhang W, Liu X, Lai L, Pei J and Li H (2017). PharmMapper 2017 update: A web server for potential drug target identification with a comprehensive target pharmacophore database. *Nucleic Acids Res.*, **45**(W1): W356-W360.

Ying Y, Nie Y, Zhao J, Dong Q, Chen M, Jiang A, Liu N, Xu T, Liu J, Pan Y, Lin L and Zhang D (2026). Periodontitis and chronic liver disease: Mechanistic insights focusing on *Porphyromonas gingivalis*—a narrative review. *Microorganisms*, **14**(4): 736.

Yu Z, Wang R, Dai T, Guo Y, Tian Z, Zhu Y, Chen J and Yu Y (2024). Identification of hub genes and key pathways in arsenic-treated rice (*Oryza sativa* L.) based on 9 topological analysis methods of CytoHubba. *Environ. Health Prev. Med.*, **29**: 41.

Zhai Y, Liu L, Zhang F, Chen X, Wang H, Zhou J, Chai K, Liu J, Lei H, Lu P, Guo M, Guo J and Wu J (2025). Network pharmacology: A crucial approach in traditional Chinese medicine research. *Chin. Med.*, **20**(1): 8.

Zhang W, Shao T, Wang C, Wang S and An L (2026). Advances in pharmacological interventions for hepatic fibrosis: From pathogenic mechanisms to novel therapeutic targets. *Ann. Med.*, **58**(1): 2613502.

Article in Press